Published in final edited form as:
Traffic. 2005 July ; 6(7): 539–547.

Analysis of the AP-2 Adaptor Complex and Cargo During Clathrin-Mediated Endocytosis

Joshua Z. Rappoport[1], **Alexandre Benmerah**[2], and **Sanford M. Simon**[1,*]

1 *The Laboratory of Cellular Biophysics, The Rockefeller University, 1230 York Avenue, PO Box 304, New York, NY 10021, USA*

2 *Department of Infectious Diseases, Institut Cochin (INSERM U567, CNRS UMR 8104, Université Paris 5), 27 rue du Faubourg St Jacques, Paris 75014, France*

Abstract

Previously, we reported that the hetero-tetrameric adaptor complex AP-2 co-localizes with the static population of clathrin spots, whereas it is excluded from clathrin spots that disappear from the plasma membrane (forming clathrin-coated vesicles). More recently however, another group provided evidence that AP-2 markers could be observed coincident with disappearing clathrin spots. Thus, we tested several possible explanations for the apparent discrepancies in these two studies. We evaluated the potential contribution of nonred emission of clathrin-dsRed (used in both studies) in the simultaneous measurement of AP-2 and clathrin at various times. Additionally, we directly compared two different green fluorescent protein-tagged AP-2 constructs (similar to those used in the previous reports). These studies demonstrated that the duration of expression time greatly influences the subcellular localization of the AP-2 markers. Furthermore, we quantitatively evaluated the AP-2 fluorescence at the sites of numerous static and disappearing clathrin spots (at least 80 per group) and confirmed our initial observation that while AP-2 is present in nearly all static clathrin spots, it is excluded from the disappearing population of clathrin spots. Finally, in order to verify that clathrin spot disappearance represents clathrin-coated vesicle internalization, we simultaneously imaged clathrin and the cargo molecule transferrin at the cell surface.

Clathrin-mediated endocytosis is a process that is evolutionarily conserved from yeast to humans and is employed in the internalization of biologically relevant cargo from the cell surface (1–6). In the quarter century since the identification of clathrin (7), numerous clathrin-associated proteins have been identified and characterized (8–12). Many of these are placed into either of two categories, adaptors or accessory proteins. The defining characteristic of an adaptor is that it binds endocytic cargo and serves as a link between the substrate for internalization and coat components (13). In contrast, accessory molecules such as dynamin seem to be involved in the complex process of endocytic vesicle formation (e.g. coat assembly or vesicular budding) without direct interaction with cargo (14,15).

The AP-2 complex was the first protein characterized as an ‘adaptor’, and it has represented the paradigm for the study of adaptor proteins (12,16–22). It is a member of the highly conserved hetero-tetrameric adaptor family or ‘APs’, and within this family, AP-2 is specifically found at the plasma membrane. It is composed of two large subunits, also called ‘adaptins’ (α and β2), and of two small subunits (μ2 and σ2). The β, μ, and σ subunits are the most highly conserved among the different APs, whereas α and its equivalents in the other complexes (γ for AP-1, δ for AP-3, and ε for AP-4) are the most divergent and therefore the most specific (10). The AP-2 complex was thought to play a central role in the formation of

*Corresponding author: Sanford M. Simon, simon@rockefeller.edu.

clathrin-coated pits (CCPs) involved in both driving the assembly of clathrin on the cytosolic leaflet of the plasma membrane and cargo selection by direct interaction with tyrosine and di-leucine-based endocytic signals (12,13,23). Additionally, the recent use of siRNA against the α and μ2 subunits has shown that the AP-2 complex is required for the formation of most, if not all, plasma membrane-associated CCPs (18,21).

The availability of clathrin light-chain constructs tagged with green fluorescent protein (GFP) or dsRed has allowed direct observation of the dynamics of clathrin in living cells [reviewed in (3)]. The use of total internal reflection fluorescence microscopy (TIR-FM) restricts the analysis to events very close to the plasma membrane and, therefore, allowed us to focus on the formation of CCPs and clathrin-coated vesicles (CCVs). The results obtained by various groups showed that clathrin spots at the plasma membrane surface can be categorized into four groups: The largest group (approximately 80%) are those that remain static during the period of observation, new spots can be observed to appear or form, approximately 2% of spots move laterally in the plane of the membrane and approximately 15% of spots disappear (all over an observation time of 60 seconds).

Those observed to disappear into the cell have been suggested to represent nascent CCVs entering the cytosol (22,24–27), probably by the effect of local actin polymerization (25). When these clathrin spots disappear, there is no alteration in the fluorescence of neighboring pixels, suggesting that the disappearance is neither due to photobleaching nor gross membrane movement into and out of the evanescent field (22,24–27). Additionally, other markers for the endocytic compartment, e.g. dynamin, have been observed to disappear at the same time, place, and rate as the clathrin spots undergoing internalization (25,27).

To better understand the dynamic of CCP formation and to more clearly identify the observed clathrin spots as CCP-derived structures, we recently generated a GFP-tagged α-adaptin construct, which was efficiently targeted to CCPs and therefore could be used as an AP-2 marker in living cells. We observed that the fluorescence intensity of clathrin and the AP-2 complex were comparable in static spots. Surprisingly, the AP-2 complex was strikingly absent from disappearing clathrin spots (22). These unexpected findings suggested that the AP-2 complex is absent from forming CCVs and drove us to propose a new model for CCP/CCV formation. In this model, the AP-2 complex would be involved in the formation of stable platforms for clathrin assembly and cargo selection from which competent CCVs could iteratively emanate. This model diverges from some previous ones that suggest each formed CCP is progressively transformed into one nascent CCV [reviewed in (3)]. However, it was recently reported that using a different GFP-tagged α-adaptin construct, AP-2 could be found in clathrin spots that disappeared from the cell surface (26). These results challenged our previous findings and the model that arose therein.

In the present study, we have evaluated potential sources of this discrepancy. This includes an analysis of the potential effects of expression time on fluorophore emission (the emission spectra of dsRed changes over time) and protein localization, a more detailed quantitative analysis of the levels of AP-2 and clathrin fluorescence in disappearing spots, and all studies were repeated with two different α-adaptin constructs. Finally, through simultaneous multicolor imaging, we have observed disappearing clathrin spots containing the endocytic cargo transferrin. These data confirm our previous observation that incorporation of AP-2 into nascent-coated vesicles is not a prerequisite for endocytosis and serve as benchmarking studies in the application of live-cell microscopy to the study of endocytosis.

Results and Discussion

Total internal reflection fluorescence microscopy (TIR-FM) produces an evanescent field that decays to 1/e in approximately 100 nm in our experimental system (28). Thus, the excitation of fluorophores decreases exponentially as a function of distance from the coverslip. As a result, the emission intensity of fluorescent endocytic markers should decrease following fission of a nascent CCV from the plasma membrane. Therefore, the observation that the fluorescence of different labeled components of the endocytic apparatus (e.g. clathrin, dynamin, etc.) that are co-localized in discrete spots disappear at the same time and same rate to background levels (in the absence of any change of fluorescence in neighboring spots) is believed to be the result of endocytosis (3,22,24–27).

Previously, using GFP-tagged α- and β2-adaptin constructs, we reported that the AP-2 complex was excluded from both the laterally mobile and the disappearing populations of clathrin spots (22). More recently, another group of investigators using the same clathrin-dsRed construct but a different GFP-tagged α-adaptin construct confirmed the absence of AP-2 from laterally mobile spots; however, this study presented data suggesting that the AP-2 complex could be found in clathrin spots disappearing from the cell surface (26).

The discrepancy between these results could be due to differences in how the experiments were performed. While we routinely image clathrin-dsRed at approximately 48-h post-transfection, the experiments in the more recent study were conducted as soon as 18-h post-transfection. This difference could be important given the previously published observation that during the initial approximately 24 h following synthesis, dsRed has a green emission (29). To test whether this could contribute to the differences in our respective observations, we transfected cells with clathrin-dsRed and quantified the relative proportion of red and green emission intensity at 18 and approximately 48-h post-transfection.

With the emission filters that we normally use for dual channel red/green imaging (515/30 and 580lp), the bleed-through of the dsRed into the green channel at 18 h was relatively minor (the ratio of 515/30 signal to 580lp was 0.65 ± 0.17%, $n = 10$ cells). However, utilizing an alternate set of emission filters (535/50 and 570lp), the emission intensity ratio of 535/50–570lp was 3.9 ± 0.5%, $n = 13$ cells. Additionally, at 44 h, this decreased to 1.0 ± 0.1%, $n = 17$ cells, a fourfold difference ($p = 7.7 \times 10^{-7}$, see Figure 1). Thus, although the absolute amount of dsRed emission collected in the green channel depends on both the expression time and the particular filters employed, situations could arise where imaging of dsRed and other fluorophores at earlier time points might not be advisable.

Another possible cause for the difference between our previous results (22) and those of Keyel et al. (26) could be due to differences in the GFP-tagged α-adaptin constructs used to follow AP-2. Indeed, in our GFP-tagged α-adaptin construct the GFP was added at the amino terminus of α-adaptin, whereas it was added to the carboxy terminus in the case of the Keyel et al. study. As these two subdomains of α-adaptin are involved in different but very important functions, it remained possible that one of the fusion proteins could be more affected than the other. To address this issue directly, we have obtained an α-adaptin construct from L. Greene similar to the one used by Keyel et al. that was previously characterized as a useful tool to follow AP-2 in live cells (30). Indeed, in our hands, this α-adaptin construct was found to efficiently localize in CCPs upon transient transfection; this α-adaptin-EGFP co-localizes with endogenous clathrin and Eps15 as well as other constitutive markers of plasma membrane CCPs (data not shown). In the present study, we have then directly compared the behavior of the two types of α-adaptin constructs in each experiment (see below).

Another possibility was that the localization and/or behaviors of α-adaptin fusion proteins change with differing expression times. As indicated above, our previous experiments were

conducted at least 40 h after transfection instead of 18 h for Keyel et al. To address this possibility, cells transiently transfected with either α-adaptin constructs (with amino- or carboxy-tagged EGFPs) were imaged at various time points following transfection. Although at 18 h, some plasma membrane-associated spots of EGFP-α-adaptin (Figure 2A,B) and α-adaptin-EGFP (data not shown) were observed, both constructs also showed strong cytoplasmic staining, even including in the nucleus (Figure 2C). In contrast, the amount of intracellular signal observed >40-h post-transfection is greatly reduced and the nuclear staining completely lost (Figure 2F, data not shown). Thus, the staining observed for both GFP-tagged α-adaptin constructs at later time points is very similar to that of endogenous AP-2, bright plasma membrane-associated puncta and faint cytosolic staining (Figures 2D,E, data not shown).

These results suggest differences in the behaviors of this fusion protein as a function of time following synthesis. They are in keeping with previous studies showing that efficient replacement of endogenous AP subunits by exogenously expressed ones require longer expression time (19,30–32) in agreement with the estimated half-life of AP-2 complexes of 24 h (33). The results also suggest that at short expression times (<18 h), the observed staining for α-adaptin is mainly due to excess monomeric forms, a possible source of artifactual observations. We have therefore chosen to analyze the behavior of both GFP-tagged α-adaptin constructs after at least 40 h of expression.

One other difference between these two studies is the way the data were evaluated and presented: our results were reported as the average amount of AP-2 present from many spots (22), while Keyel et al. showed images from representative events (26). One manuscript presented a quantification of AP-2 relative to clathrin, and the other reported whether or not AP-2 could be detected co-localizing with clathrin. The question we address is whether there is a significant quantitative difference in the amount of AP-2 co-localizing with static and disappearing clathrin spots. We addressed this question by quantitatively analyzing numerous static and disappearing clathrin-dsRed spots in cells co-expressing either the same construct used in our previous paper or the carboxy terminal tagged α-adaptin. In these studies, data were analyzed from 12-bit images (technical constraints had limited our previous study to 8 bits). Additionally, we have extended our studies to numerous data points (at least 80 spots from at least 12 cells per group).

Cells were transiently transfected with clathrin-dsRed and GFP-tagged α-adaptin constructs, imaged 44–48 h later, and static and disappearing clathrin spots were selected. These studies verified that markers for the AP-2 complex were largely absent from the disappearing population of clathrin (Figure 3 and Video 1 available online at http://www.traffic.dk/suppmat/6_7.asp), as previously reported (3,22). Additionally, disappearing clathrin spots can be observed to apparently emanate from static co-localized clathrin/AP-2 spots (Figure 4), further illustrating our previous observation that the static (AP-2 positive) and active (AP-2 negative) populations of clathrin are not completely distinct (22). Given that in these image streams acquisition time is limited to approximately 30 seconds, the average time for clathrin spot disappearance is approximately 17.5 seconds (27), and clathrin spots move at approximately 1 μm per second (34), it is not surprising that this behavior was not observed for each disappearing clathrin spot identified.

To quantify these results, averages were calculated for the amount of red (clathrin-dsRed) or green (GFP-α-adaptin) intensity for 106 static or disappearing spots (Figure 3). The intensity data were normalized by dividing the average intensity value for each spot by the average intensity within an annulus surrounding it and then subtracting ‘one’. Consistent with our previous results, the AP-2 intensity relative to local background was higher in the static spots (0.59 ± 0.04) than in the disappearing spots(0.10 ± 0.02) ($p = 3.6 \times 10^{-21}$) (Figure 5A). In

contrast, the difference between the intensity of clathrin in the static (0.65 ± 0.04) and disappearing (0.53 ± 0.03) spots was much smaller ($p = 0.02$). Although the amount of clathrin and AP-2 in static spots were statistically indistinguishable ($p = 0.34$), the amount of clathrin in disappearing spots was significantly greater than the amount of AP-2 ($p = 3.2 \times 10^{-25}$).

An alternate way of viewing these data is to quantify the ratio of clathrin to AP-2 in the different populations of spots. Although this will not permit an evaluation of the numbers of molecules per spot due to unknown extent of labeling as well as the contributions of the different quantum yields of the fluorophores being used, this ratio permits a further illustration of the differences between the static and disappearing spots. The ratio of clathrin to AP-2 for each group was calculated and compared between the static and disappearing populations (Figure 5B). Consistent with the previous analyses, the ratio of clathrin to AP-2 in static spots (1.04) was much closer to unity than in disappearing spots (5.3). These experiments and quantifications were repeated with the α-adaptin construct with EGFP on the carboxy terminus in 82 static and disappearing spots, and the results were not qualitatively different than that shown in Figure 5 (supplementary figure 1 available online at http://www.traffic.dk/suppmat/6_7.asp).

A histogram was made of the ratio of AP-2 fluorescence over background in static and disappearing spots (Figure 6A). The majority of disappearing spots contain AP-2 intensities very close to local background (81% in the first subdivision), while 79% of static spots contain AP-2 higher than local background (above the first subdivision). The histogram of the ratio of clathrin to AP-2 (Figure 6B) shows that approximately 75% of static spots contain equivalent amounts of clathrin and AP-2 (fall within the first two subdivisions), while only approximately 10% of disappearing spots were within this same range. Furthermore, 57% of disappearing clathrin spots contained clathrin/AP-2 ratios greater than six, including those values with AP-2 intensities at or below local background. Additionally, the analysis of the results obtained with the carboxy tagged α-adaptin produced similar results (supplementary figure 2 available online at http://www.traffic.dk/suppmat/6_7.asp).

We have previously observed the co-localization of Tf with plasma membrane-associated clathrin-dsRed in fixed cells (27). We next tested whether endocytic cargo was co-localized with the static or dynamic clathrin spots in living cells. We have used two different approaches to study the endocytosis of cargo. One approach is to perfuse cells with fluorescent-labeled cargo and image cargo bound to the surface with a background of free diffuse cargo. The second approach is to cool cells down to block receptor-mediated endocytosis, load fluorescent-tagged cargo in the cold, and then wash away excess cargo before warming up the cell. One study has been published utilizing the former approach and cargo was observed to disappear from the evanescent field (26). However, neither clathrin nor other components of the endocytic machinery were simultaneously labeled. Thus, it was not determined whether these ligand-containing structures reflected nascent clathrin-coated endocytic vesicles. Additionally, this methodology resulted in a strong, diffuse background haze of free ligand in the imaging media (26), an observation also obtained in our preliminary studies (data not shown).

Cells were cooled on ice, in the cold room (4 °C), and incubated with transferrin, a cargo molecule that uses the clathrin-mediated endocytic pathway (17–19,21,35). Cells were imaged after warming to 32 °C, in the presence of prewarmed imaging medium. Transferrin was observed to co-localize spatially and temporally with both static and disappearing clathrin spots (Figures 7C,D and Video 2 available online at http://www.traffic.dk/suppmat/6_7.asp). When the fluorescence at a particular co-localized spot was observed to disappear, the transferrin fluorescence would start to disappear at the same time and disappeared at the same rate (Figure 7E). These results are consistent with the assumption that the disappearance of a clathrin spot from the evanescent field is the result of clathrin-mediated endocytosis. Thus, these images

represent the first direct quantitative observation of the internalization of cargo-containing clathrin-coated structures into a living cell.

While this manuscript was in review, Ehrlich et al. (36) published findings that AP-2 was present in disappearing clathrin-coated vesicles. This study presented a quantitative analysis of σ2-adaptin in BSC1 cells via time-lapse spinning disk confocal microscopy (36). One potential explanation may rest with the choice of marker for AP-2. In our studies, we used labeled α or β2 adaptin [this work and (22)], which we have shown to be co-localized with native AP-2 during the time periods of expression we used. Ehrlich et al. used a labeled σ2-adaptin. A significant portion of the labeled σ2-adaptin was found in the nucleus and did not appear to co-localize with native AP-2. A second explanation is that the choice of instrumentation and time period of acquisition required by the instrumentation is likely to have a significant effect. The studies of Ehrlich et al. used a spinning-disk confocal microscope and alternated between collecting images of AP-2 and clathrin. This resulted in a maximum frame rate for each protein of one image every 5.2 seconds. Our total internal reflection microscope system allowed the simultaneous imaging of AP-2 and clathrin every 0.2 seconds. This increased sampling rate may have provided for the detection of more rapid clathrin dynamics than would otherwise remain undetected.

Indeed, some of the observations in the Ehrlich paper are consistent with our own. A histogram of lifetimes showed that AP-2 was on the surface of the cell 6 s shorter than clathrin (Figure 2) (36). However, in Figure 4 (36), they show AP-2 and clathrin on the surface for equivalent periods but only after they had preselected for events that were on the surface ‘each with a lifetime of 42 seconds’. It is also our impression that in Figure 6 there is clear demonstration of a diffraction-limited spot emanating from stable clusters (the spot marked by the upper arrow). While this is not the interpretation of the authors, we believe it is consistent with our previous work and that of others (22,24,37).

In conclusion, our new results are consistent with our previous observation (22) that there is a clear distinction between the AP-2 content in static versus disappearing clathrin spots. These disappearing spots contain endocytic cargo (Figure 7) but have reduced AP-2 relative to static plasma membrane domains. These observations suggest that the AP-2 complex is excluded, at least beyond our limits of detection, from the vast majority of nascent endocytic vesicles. One important point to be resolved is the origin(s) of the different populations of plasma membrane associated clathrin. Are the static, disappearing, and laterally mobile spots similar structures at different points in a shared natural history or are they completely independent entities? Do static clathrin spots that contain both AP-2 and clathrin serve as platforms for the assembly of active disappearing spots? If so, for how many cycles? Is all the AP-2 excluded from coated vesicles or is a substoichiometric amount retained upon budding? These issues emphasize the importance of quantification of the observed phenomenon and furthermore provide support for the constant need for technological advancement in data acquisition and re-evaluation of data analysis.

Experimental Procedures

Plasmid constructs and cell culture

Clathrin-dsRed was a gift of Dr Tomas Kirchhausen, Harvard Medical School, Boston, MA, USA. Rat α-adaptin-EGFP was a gift of Dr Lois Greene, National Institutes of Health, Bethesda, MD, USA. The production of mouse EGFP-α-adaptin was described previously (22). HeLa cells were maintained in DMEM (Mediatech Cellgro, Herndon, VA, USA) with 10% FBS in a 37 °C incubator humidified with 5% CO_2 and were imaged 18 or approximately 48-h after transfection with Fugene6 (Roche Diagnostics, Indianapolis, IN, USA).

Cell surface Tf labeling

Cells plated on MatTek 35-mm dishes (part no. P35G-1.5–10-C, MatTek Corp., Ashland, MA, USA) were rinsed in warm serum-free DMEM (SFM) and placed in SFM for 30 min in a 37 °C incubator to chase out cell surface-bound Tf. Cells were rinsed in ice cold PBS and placed on ice at 4 °C for 15 min in AlexaFluor488-Tf (Molecular Probes, Eugene, OR, USA) diluted 1:100 in PBS. Cells were rinsed in ice cold PBS and placed onto the microscope stage (32 ° C). Two milliliters of prewarmed imaging media were added and imaging was immediately begun.

Total internal reflection fluorescence microscopy image acquisition

Total internal reflection fluorescence microscopy was performed as previously described using the following microscope objective: Apo 60X NA 1.45 Olympus America Inc. (Melville, NY, USA) (22,27,34,38). Clathrin-dsRed and Alexa488-Tf imaging were performed at 32 °C. Excitation was performed with the 488-nm line of a tunable argon laser (Omnichrome, model 543-AP A01, Melles Griot, Carlsbad, CA, USA) and a 543-nm HeNe laser (model 05-LGR-193, Melles Griot) reflected off a 488/543 polychroic mirror. All mirrors and filters were obtained from Chroma Technologies Corp. (Brattleboro, VT, USA). Clathrin-dsRed and EGFP-α-adaptin (or α-adaptin-EGFP) were imaged at 37 °C. For these constructs, excitation was performed with the 488-nm line as above reflected off a 498 dichroic mirror. In all cases, green and red emissions were collected simultaneously using a Dual-View splitter (Optical Insights, Santa Fe, NM, USA) equipped with a 515/30 band-pass filter to collect green emission, a 550 dichroic to split the emission, and a 580 long-pass filter to collect red emission. Streams of 100–300 frames were acquired at 100–300 ms per frame.

Dual-color processing

Following the subtraction of extra-cellular background, 12-bit dual-color TIR-FM image streams were aligned using a journal written for MetaMorph (Universal Imaging, Downingtown, PA). On the basis of preliminary single fluorophore control experiments, green to red bleed-through corrections of 25% for Alexa488-Tf and clathrin-dsRed and 10% for EGFP-α-adaptin (or α-adaptin-EGFP) and clathrin-dsRed were employed.

Calculation of fluorescence in disappearing and static spots

For EGFP-α-adaptin, a total of 106 disappearing and 106 static spots were identified from 13 cells, and for α-adaptin-EGFP, a total of 82 disappearing and 82 static spots were identified from 12 cells. Clathrin spots were identified as static if they neither moved laterally nor into the cell during the entire length of the acquired image stream. Disappearing spots were selected for analysis if the intensity at that point decreased to background during the time of imaging without being due to lateral displacement, photobleaching, or cell/membrane movement. In each case following the identification of each disappearing spot, the nearest static spot of roughly comparable apparent size and intensity was selected so that the effects of local phenomena would be minimized.

Once static and disappearing spots were identified, the total fluorescence and area of the region of interest were obtained for each spot in each channel, as were the total fluorescence and area of a larger region surrounding each spot. We quantified the values from the very first time point of each sequence. This was done for two reasons. First, to avoid potential problems of differential photo-bleaching between dsRed and EGFP, and second, because the fluorescence is decreasing as the puncta disappear, the signal to noise is substantially increasing. Thus, we are contrasting the fluorescence from clathrin and AP-2 from spots that either remain static or will disappear during the subsequent sequence and not the fluorescence during the disappearance. The total fluorescence and area of the spot were subtracted from the values for

the larger region, and then the resultant fluorescence was divided by the area to obtain a value for average background fluorescence within an annulus surrounding each spot. Finally, the fluorescence intensity for each spot was normalized relative to local background by dividing the average spot fluorescence per pixel by the average annulus fluorescence per pixel and then subtracting 1 from each value. The histogram analysis for the ratio of clathrin/AP-2 placed all values with AP-2 intensity at or below local background within the final subdivision (>6).

Supplementary Material

Refer to Web version on PubMed Central for supplementary material.

Acknowledgements

This work was supported by NIH 1 F32 G069200-01 (J.Z.R.), 'Association pour la Recherche contre le Cancer' 4727 (A.B.), and NSF BES-0110070 and BES-0119468 (S.M.S.). The authors thank Florence Koeppel, Marina Fix, and Shahrnaz Kemal for the critical evaluation of this manuscript.

References

1. Baggett JJ, Wendland B. Clathrin function in yeast endocytosis. Traffic 2001;2:297–302. [PubMed: 11350625]
2. Geli MI, Riezman H. Endocytic internalization in yeast and animal cells. similar and different. J Cell Sci 1998;111 (8):1031–1037. [PubMed: 9512499]
3. Rappoport J, Simon S, Benmerah A. Understanding living clathrin-coated pits. Traffic 2004;5:327–337. [PubMed: 15086782]
4. Schmid SL. Clathrin-coated vesicle formation and protein sorting: an integrated process. Annu Rev Biochem 1997;66:511–548. [PubMed: 9242916]
5. Brodsky FM, Chen CY, Knuehl C, Towler MC, Wakeham DE. Biological basket weaving: formation and function of clathrin-coated vesicles. Annu Rev Cell Dev Biol 2001;17:517–568. [PubMed: 11687498]
6. Conner SD, Schmid SL. Regulated portals of entry into the cell. Nature (Lond) 2003;422:37–44. [PubMed: 12621426]
7. Pearse BM. Clathrin: a unique protein associated with intracellular transfer of membrane by coated vesicles. Proc Natl Acad Sci USA 1976;73:1255–1259. [PubMed: 1063406]
8. Brett TJ, Traub LM, Fremont DH. Accessory protein recruitment motifs in clathrin-mediated endocytosis. Structure (Camb) 2002;10:797–809. [PubMed: 12057195]
9. Brooksbank C. Endocytosis. Tent pegs for clathrin. Nat Rev Mol Cell Biol 2001;2:166. [PubMed: 11265244]
10. Kirchhausen T. Adaptors for clathrin-mediated traffic. Annu Rev Cell Dev Biol 1999;15:705–732. [PubMed: 10611976]
11. Kirchhausen T. Clathrin adaptors really adapt. Cell 2002;109:413–416. [PubMed: 12086597]
12. Traub LM. Sorting it out: AP-2 and alternate clathrin adaptors in endocytic cargo selection. J Cell Biol 2003;163:203–208. [PubMed: 14581447]
13. Kirchhausen T, Bonifacino JS, Riezman H. Linking cargo to vesicle formation: receptor tail interactions with coat proteins. Curr Opin Cell Biol 1997;9:488–495. [PubMed: 9261055]
14. Altschuler Y, Barbas SM, Terlecky LJ, Tang K, Hardy S, Mostov KE, Schmid SL. Redundant and distinct functions for dynamin-1 and dynamin-2 isoforms. J Cell Biol 1998;143:1871–1881. [PubMed: 9864361]
15. Praefcke GJ, McMahon HT. The dynamin superfamily: universal membrane tubulation and fission molecules? Nat Rev Mol Cell Biol 2004;5:133–147. [PubMed: 15040446]
16. Benmerah A, Lamaze C, Begue B, Schmid SL, Dautry-Varsat A, Cerf-Bensussan N. AP – 2/Eps15 interaction is required for receptor-mediated endocytosis. J Cell Biol 1998;140:1055–1062. [PubMed: 9490719]

17. Conner SD, Schmid SL. Differential requirements for AP-2 in clathrin-mediated endocytosis. J Cell Biol 2003;162:773–779. [PubMed: 12952931]
18. Hinrichsen L, Harborth J, Andrees L, Weber K, Ungewickell EJ. Effect of clathrin heavy chain- and alpha-adaptin-specific small inhibitory RNAs on endocytic accessory proteins and receptor trafficking in HeLa cells. J Biol Chem 2003;278:45160–45170. [PubMed: 12960147]
19. Huang F, Khvorova A, Marshall W, Sorkin A. Analysis of clathrin-mediated endocytosis of EGF receptor by RNA interference. J Biol Chem 2004;279:16657–16661. [PubMed: 14985334]
20. Mishra SK, Watkins SC, Traub LM. The autosomal recessive hypercholesterolemia (ARH) protein interfaces directly with the clathrin-coat machinery. Proc Natl Acad Sci USA 2002;99:16099–16104. [PubMed: 12451172]
21. Motley A, Bright NA, Seaman MN, Robinson MS. Clathrin-mediated endocytosis in AP-2-depleted cells. J Cell Biol 2003;162:909–918. [PubMed: 12952941]
22. Rappoport JZ, Taha BW, Lemeer S, Benmerah A, Simon SM. The AP-2 complex is excluded from the dynamic population of plasma membrane-associated clathrin. J Biol Chem 11–28 2003;278:47357–47360.
23. Robinson MS. Adaptable adaptors for coated vesicles. Trends Cell Biol 2004;14:167–174. [PubMed: 15066634]
24. Gaidarov I, Santini F, Warren RA, Keen JH. Spatial control of coated-pit dynamics in living cells. Nat Cell Biol 1999;1:1–7. [PubMed: 10559856]
25. Merrifield CJ, Feldman ME, Wan L, Almers W. Imaging actin and dynamin recruitment during invagination of single clathrin-coated pits. Nat Cell Biol 2002;4:691–698. [PubMed: 12198492]
26. Keyel PA, Watkins SC, Traub LM. Endocytic adaptor molecules reveal an endosomal population of clathrin by total internal reflection fluorescence microscopy. J Biol Chem 2004;279:13190–13204. [PubMed: 14722064]
27. Rappoport JZ, Simon SM. Real-time analysis of clathrin mediated endocytosis during cell migration. J Cell Sci 2003;116:847–855. [PubMed: 12571282]
28. Lampson MA, Schmoranzer J, Zeigerer A, Simon SM, McGraw TE. Insulin-regulated Release from the Endosomal Recycling Compartment Is Regulated by Budding of Specialized Vesicles. Mol Biol Cell 2001;12:3489–3501. [PubMed: 11694583]
29. Baird GS, Zacharias DA, Tsien RY. Biochemistry, mutagenesis, and oligomerization of DsRed, a red fluorescent protein from coral. Proc Natl Acad Sci USA 2000;97:11984–11989. [PubMed: 11050229]
30. Wu X, Zhao X, Puertollano R, Bonifacino JS, Eisenberg E, Greene LE. Adaptor and Clathrin Exchange at the Plasma Membrane and trans-Golgi Network. Mol Biol Cell 2003;14:516–528. [PubMed: 12589051]
31. Gaidarov I, Keen JH. Phosphoinositide–AP –2 interactions required for targeting to plasma membrane clathrin-coated pits. J Cell Biol 1999;146:755–764. [PubMed: 10459011]
32. Nesterov A, Carter RE, Sorkina T, Gill GN, Sorkin A. Inhibition of the receptor-binding function of clathrin adaptor protein AP-2 by dominant-negative mutant mu2 subunit and its effects on endocytosis. EMBO J 1999;18:2489–2499. [PubMed: 10228163]
33. Sorkin A, McKinsey T, Shih W, Kirchhausen T, Carpenter G. Stoichiometric interaction of the epidermal growth factor receptor with the clathrin-associated protein complex AP-2. J Biol Chem 1995;270:619–625. [PubMed: 7822287]
34. Rappoport JZ, Taha BW, Simon SM. Movement of plasma-membrane-associated clathrin spots along the microtubule cytoskeleton. Traffic 2003;4:460–467. [PubMed: 12795691]
35. Benmerah A, Bayrou M, Cerf-Bensussan N, Dautry-Varsat A. Inhibition of clathrin-coated pit assembly by an Eps15 mutant. J Cell Sci 1999;112 (9):1303–1311. [PubMed: 10194409]
36. Ehrlich M, Boll W, Van Oijen A, Hariharan R, Chandran K, Nibert ML, Kirchhausen T. Endocytosis by random initiation and stabilization of clathrin-coated pits. Cell 2004;118:591–605. [PubMed: 15339664]
37. Yarar D, Waterman-Storer CM, Schmid SL. A Dynamic Actin Cytoskeleton Functions at Multiple Stages of Clathrin-mediated Endocytosis. Mol Biol Cell 2004;16:964–975. [PubMed: 15601897]
38. Schmoranzer J, Goulian M, Axelrod D, Simon SM. Imaging constitutive exocytosis with total internal reflection fluorescence microscopy. J Cell Biol 2000;149:23–32. [PubMed: 10747084]

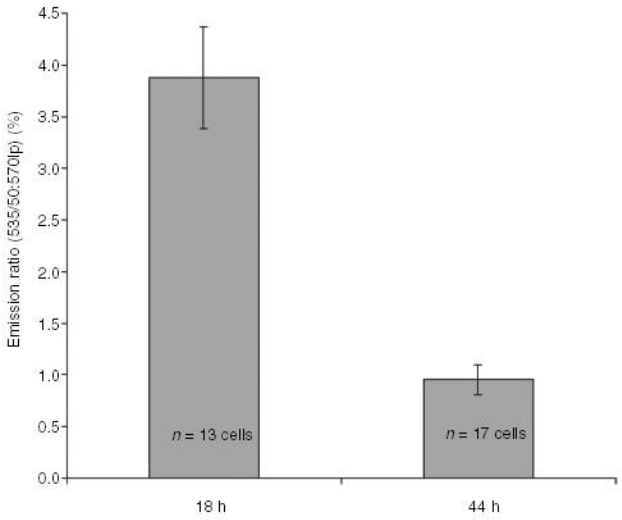

Figure 1. Analysis of clathrin-dsRed emission over time

The emission intensity from total internal reflection fluorescence microscopy images was compared between 13 cells expressing clathrin-dsRed at 18-h post-transfection and 17 cells at 44 h. The mean ± SEM is presented for the ratio of emission between 510 and 560 nm and that above 570 nm.

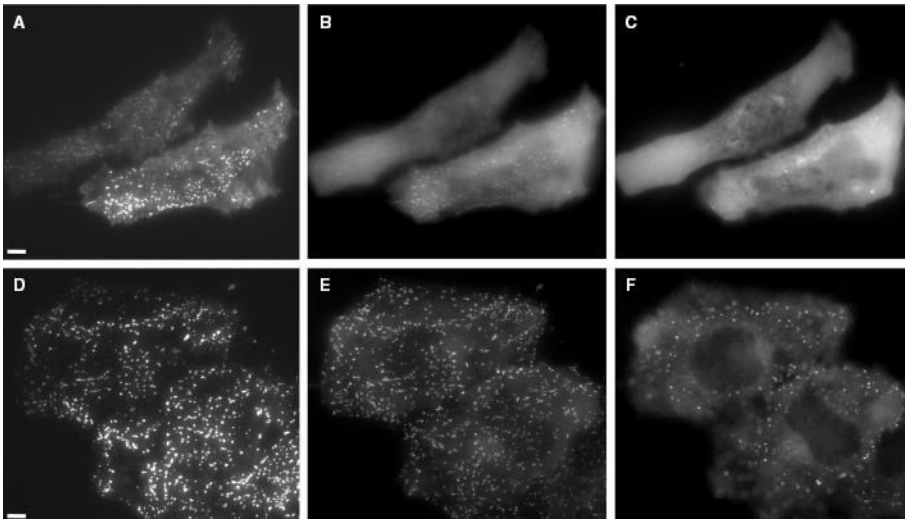

Figure 2. Localization of EGFP-α-adaptin over time

The subcellular localization of the EGFP-α-adaptin construct was documented at 18- (A, B, and C) and 44-h (D, E, and F) post-transfection. Images were obtained via total internal reflection fluorescence microscopy (A and D) as well as epi-fluoresence at both the cell surface (B and E) and within the cytosol (C and F). Scale bars equal 5 μm.

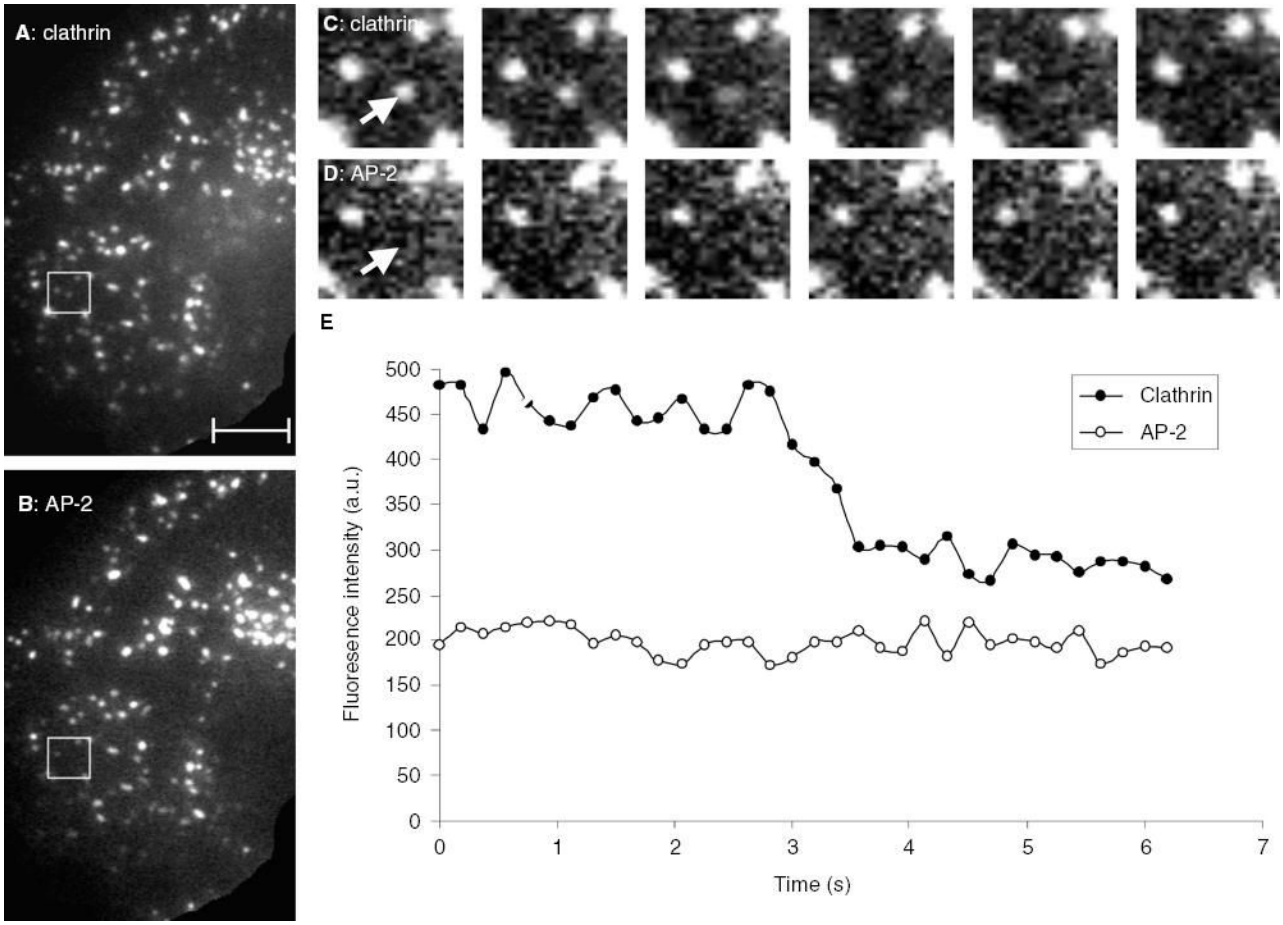

Figure 3. Absence of AP-2 from disappearing clathrin spots

HeLa cells transfected with A) clathrin-dsRed and B) EGFP-α-adaptin were imaged by total internal reflection fluorescence microscopy. Sequential images from video acquired at 190 ms/frame demonstrate that although most clathrin spots C) co-localize with AP-2, D) the spot that undergoes internalization from the cell surface (marked by the arrow) does not. Quantification of fluorescence intensity of the disappearing spot shown in C) and D) is presented in E). Scale bars equal 5 μm.

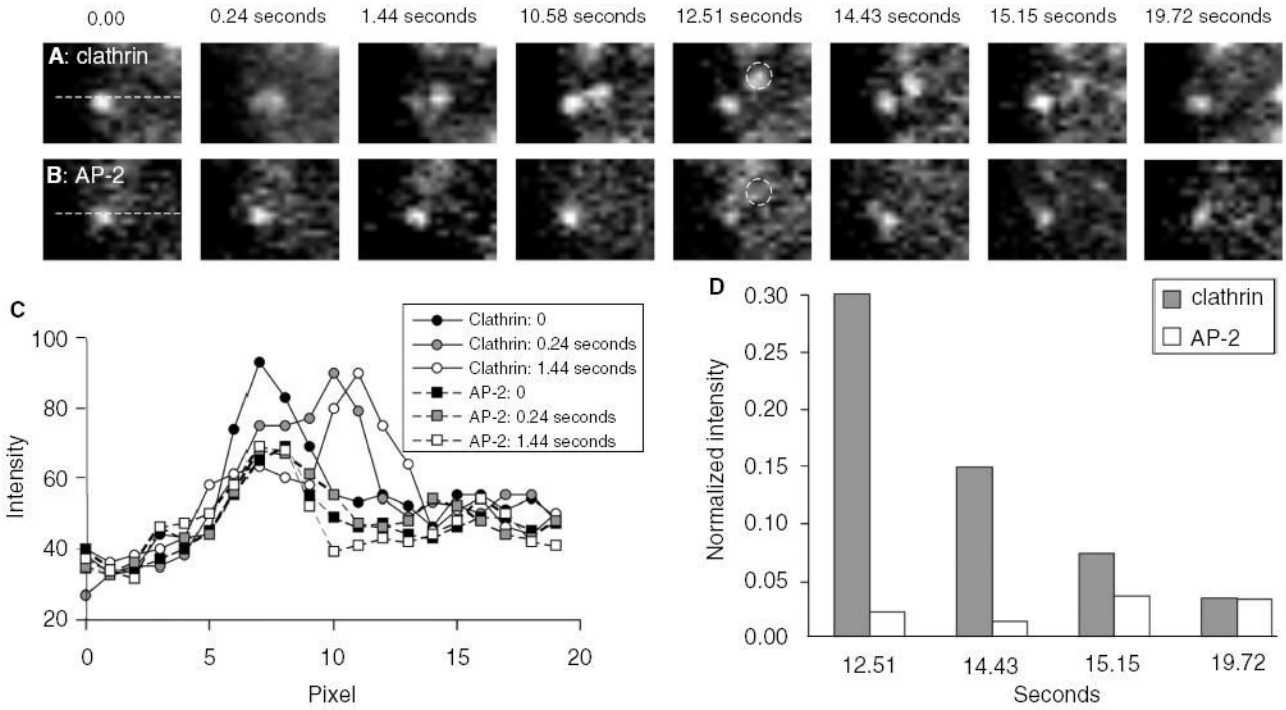

Figure 4. Absence of AP-2 from disappearing clathrin spot that appears to split from co-localized clathrin/AP-2 spot

HeLa cells transfected with A) clathrin-dsRed and B) EGFP-α-adaptin were imaged by total internal reflection fluorescence microscopy acquired at approximately 240 ms/frame. The clathrin spot that originates at the site of co-localized clathrin and AP-2 and subsequently moves away and disappears, does not contain AP-2. Quantifications of fluorescence intensity along the line in A) and B), presented in C), demonstrates the absence of AP-2 from the portion that separates off from the static co-localized spot. Quantification of the disappearance of the clathrin spot marked by the circles in A) and B) is presented in D). The area of the region of interest in A) and B) is $2.52 \times 1.86\ \mu m^2$.

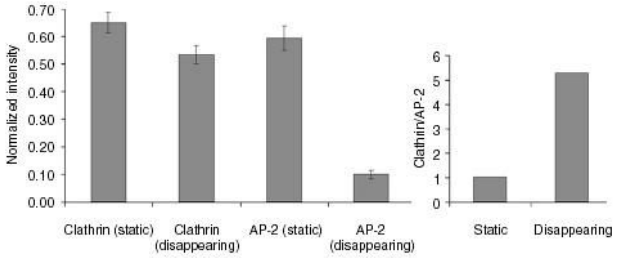

Figure 5. Clathrin and AP-2 at the sites of static and disappearing spots

The clathrin-dsRed and EGFP-α-adaptin intensities relative to local background were measured from 106 disappearing and static clathrin spots. A) The mean ± SEM of intensity divided by local background, including subtraction of the number '1' to normalize for local background. B) The ratio of the mean clathrin intensity divided by mean AP-2 intensity for the 106 disappearing and static clathrin spots from A).

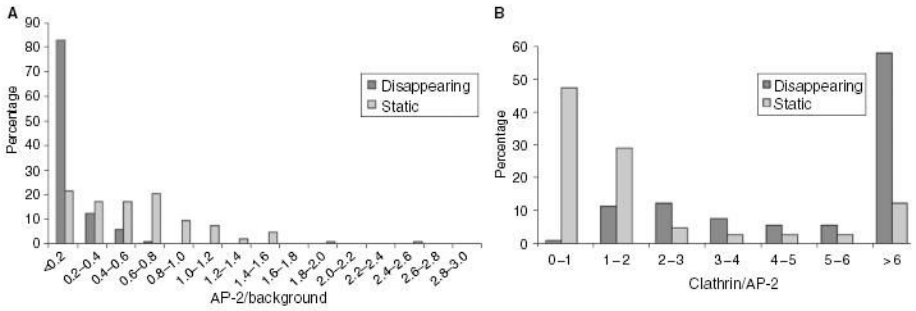

Figure 6. Histograms of clathrin and AP-2 at the sites of static and disappearing spots

The distributions of the clathrin-dsRed and EGFP-α-adaptin intensities relative to local background are presented from 106 disappearing and static clathrin spots. A) Histogram of AP-2 intensity divided by local background, including subtraction of the number '1' to normalize for local background. B) Histogram of the ratio of clathrin relative to local background divided by AP-2 relative to local background.

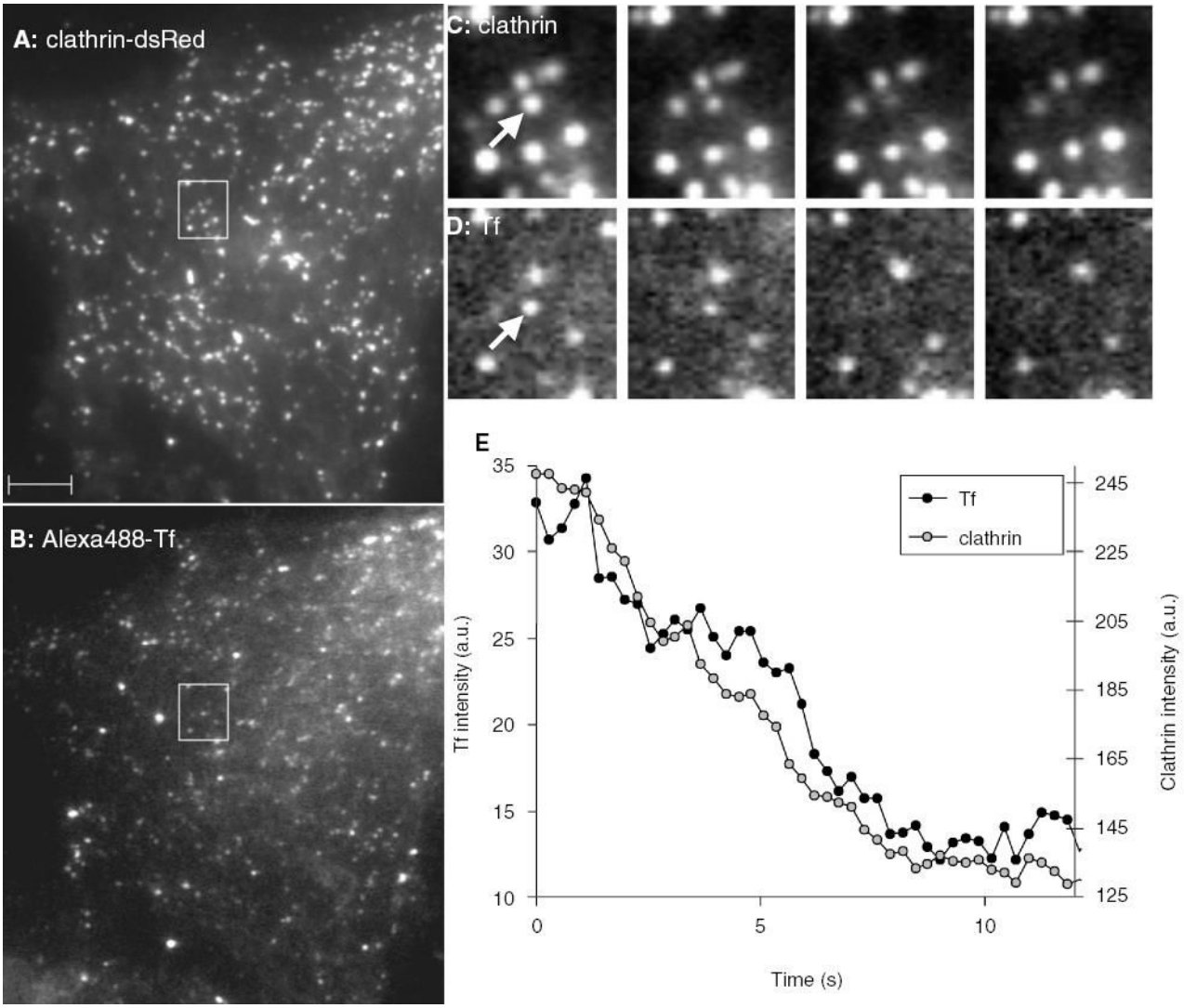

Figure 7. Co-localization of Tf in disappearing clathrin spots

HeLa cells transfected with A) clathrin-dsRed and incubated in the cold in the presence of B) Alexa488-Tf were imaged by total internal reflection fluorescence microscopy. Images from video acquired at 280 ms/frame and shown every 10 frames demonstrate the simultaneous disappearance of C) clathrin and D) Tf. Quantification of fluorescence intensity of the disappearing spots shown in C) and D) is presented in E). Scale bars equal 5 μm.